Wood Science and Technology (2025) 59:13
https://doi.org/10.1007/s00226-024-01620-8

ORIGINAL

Progressive degradation of acetylated wood by the brown rot fungi *Coniophora puteana* and *Rhodonia placenta*

Tiina Belt[1] · **Muhammad Awais**[2,3]

Received: 4 July 2024 / Accepted: 7 November 2024

Abstract

Acetylation is a wood modification method that reduces the hygroscopicity of wood and increases its resistance to degradation by wood decaying fungi. Even though acetylated wood can have very high decay resistance, the wood material can be degraded and sometimes deacetylated by fungi. This study investigated the degradation and deacetylation of acetylated wood by *Coniophora puteana* and *Rhodonia placenta* to better understand the relationship between degradation and deacetylation in two different brown rot fungi. Wood samples were exposed to the fungi in a stacked-sample decay test, followed by acetyl content measurements and FTIR spectroscopy to investigate chemical changes in the samples. The results showed that both fungi could degrade acetylated wood to high mass loss despite a strong reduction in moisture content, but only *R. placenta* was found to cause preferential deacetylation. The deacetylation was slight and only observed in the early stages of decay in highly acetylated wood. Otherwise, acetyl groups were lost from the samples at the rate of mass loss. FTIR spectroscopy confirmed the loss of acetyl groups and revealed some chemical differences between unacetylated and acetylated wood. The spectral data indicated the loss of acetyl groups from lignin, which suggests that the loss of acetyl groups is not only due to the degradation of acetylated carbohydrates. The degradation of acetylated wood required further investigation, but it is clear that extensive deacetylation is not a requirement for brown rot degradation.

✉ Tiina Belt
tiina.belt@luke.fi

[1] Natural Resources Institute Finland, Production Systems Unit, Viikinkaari 9, Helsinki 00790, Finland

[2] Norwegian University of Life Sciences, Faculty of Science and Technology, Pb 5003, Ås 1433, Norway

[3] School of Chemical Engineering, Department of Bioproducts and Biosystems, Aalto University, P.O. Box 16300, Aalto 00076, Finland

Published online: 19 November 2024

Introduction

Wood modification is a term that describes a range of treatments that improve the properties of wood by a nontoxic mode of action (Hill 2006). Acetylation is one of the most extensively studied wood modifications methods, and it involves the reaction of wood with acetic anhydride, resulting in the incorporation of acetyl esters in the wood cell wall. The added acetyl groups occupy space in the cell wall, reducing the moisture content of wood primarily by cell wall bulking (Papadopoulos and Hill 2003; Thybring et al. 2020). Acetylation reduces the moisture content of the wood cell walls in the hygroscopic (Himmel and Mai 2015; Čermák et al. 2022) and over-hygroscopic moisture range (Thygesen et al. 2010; Fredriksson et al. 2024) and at full water saturation (Hill et al. 2005; Beck et al. 2018d; Digaitis et al. 2021), and it changes the interaction of the cell walls with capillary water (Beck et al. 2018d; Digaitis et al. 2021; Fredriksson et al. 2024).

Acetylation also improves the resistance of the wood material to degradation by wood decaying fungi. Although the mechanisms behind improved decay resistance are not fully understood, it is thought that the improvement is due to the reduction in moisture content, which interferes with the diffusion of fungal degradative agents (Thybring 2013; Ringman et al. 2014, 2019; Zelinka et al. 2016). Very high decay resistance is usually achieved at around 20% weight percent gain (WPG) due to modification, which corresponds to an approx. 40% reduction in cell wall moisture content and a decrease in maximum cell wall moisture content to below 25% (Thybring 2013). However, even though acetylation greatly improves decay resistance, several studies have shown that even high WPG acetylated wood will decay if exposed to fungi under suitable conditions for a sufficiently long period of time (Hill et al. 2006; Beck et al. 2018a, c; Thygesen et al. 2021; Ponzecchi et al. 2024). Some studies utilising the brown rot fungus *Rhodonia placenta* have detected deacetylation of the acetylated wood (Beck et al. 2018c; Ponzecchi et al. 2024), which may explain how the initially highly resistant material becomes degradable. However, the results on whether deacetylation takes place and to what extent are conflicting. Ringman et al. (2017) detected no deacetylation in acetylated wood exposed to *R. placenta*, while Thygesen et al. (2021) detected deacetylation by FTIR spectroscopy but not by Raman spectroscopy imaging. Furthermore, no data exist for fungi other than *R. placenta*.

To gain more insight into the degradation of acetylated wood, this study investigated the degradation and deacetylation of acetylated wood by two different brown rot fungi. Scots pine samples acetylated to two different WPGs were exposed to the previously studied *R. placenta* as well as *Coniophora puteana* in a stacked-sample decay test to generate samples in different stages of decay. Mass losses and moisture contents were measured, after which deacetylation and chemical changes were investigated by saponification and FTIR spectroscopy. The objectives were to determine if (1) both fungi can cause substantial degradation in acetylated wood, (2) both fungi can deacetylate acetylated wood, and (3) degradation produces similar chemical changes in acetylated wood to unmodified wood.

Materials and methods

Sample preparation

Samples with dimensions 8 mm x 8 mm x 12 mm (longitudinal x tangential x radial) were sawn from commercial kiln dried boards of Scots pine (*Pinus sylvestris*) sapwood. The samples were Soxhlet extracted (6 h) with acetone to remove acetone-soluble extractives and then oven dried at 105 °C for 24 h to determine their initial dry mass. Two sets of samples were acetylated in neat acetic anhydride, while one set of samples was left unmodified to act as reference. The samples to be acetylated were first impregnated with the anhydride at room temperature (under vacuum for 2 h, followed by soaking in the anhydride overnight at atmospheric pressure) and then acetylated in fresh anhydride at 120 °C for 20 min or 6 h. After reaction the treatment flasks were cooled in an icebath and the anhydride replaced with acetone. The modified samples were soaked in acetone overnight and then Soxhlet extracted again with acetone to remove reaction by-products and unreacted anhydride. Finally, the samples were dried at 105 °C for 24 to determine their modified dry mass. WPG due to modification was calculated according to Eq. 1:

$$WPG\ (\%) = \frac{m_{mod} - m_{init}}{m_{init}} \times\ 100\% \tag{1}$$

where m_{init} is the initial dry mass of the samples, and m_{mod} is the modified dry mass of the samples.

The samples acetylated for 20 min and 6 h reached an average WPG of 9.3 (±0.7)% and 18.4 (±0.5)%, respectively. After drying the acetylated and unmodified reference samples were sterilised by ionising radiation (25–50 kGy dose) and then conditioned at 85% RH over a saturated solution of KCl at room temperature for 3 months.

Decay test

The decay test was performed using a similar setup as in Belt et al. (2022). Four ml of 2% malt extract agar medium were added to 16-mm-diameter test tubes and inoculated with one plug of mycelium from the growing edges of *C. puteana* (strain BAM Ebw. 15) or *R. placenta* (strain BAM 113) stock cultures maintained on 2% malt extract agar. A piece of plastic netting was placed over the mycelial plug, followed by 6 wood samples stacked on top of each other. The tubes were plugged with cotton wool and incubated at 85% RH over a saturated solution of KCl at room temperature. As the objective of the decay test was to produce a range of mass losses in every sample type (reference, 9% WPG, and 18% WPG), the different sample types were incubated with the two fungi for different durations. All replicate tubes (7 for all sample types exposed to *C. puteana* and 5 for all sample types exposed to *R. placenta*) corresponding to one sample type-fungus combination were removed from the test when the visible fungal mycelium had reached the top of the topmost block in one replicate tube. The samples were removed from the tubes, brushed to remove adhering mycelium and weighed to determine their decaying wet mass. The samples

were dried overnight under a fume hood and then at 105 °C for 24 h to determine their decayed dry mass. For each sample, mass loss (ML), moisture content (MC) at the end of the decay test, and moisture content corrected for WPG and mass loss at the end of the decay test (MC*) were calculated according to Eqs. 2–4:

$$ML\ (\%) = \frac{m_{undec} - m_{dec}}{m_{undec}} \times\ 100\% \tag{2}$$

$$MC\ (\%) = \frac{m_{wet} - m_{dec}}{m_{dec}} \times\ 100\% \tag{3}$$

$$MC^{*}\ (\%) = \frac{m_{wet} - m_{dec}}{m_{init}} \times\ 100\% \tag{4}$$

where m_{undec} is the undecayed dry mass of the samples (m_{init} for references and m_{mod} for modified samples), m_{dec} is the decayed dry mass of the samples, and m_{wet} is the decaying wet mass of the samples.

After the decay test, a total of 15 samples from every type-fungus combination were selected for further analysis based on their mass loss. The samples were ground in a laboratory knife mill (IKA A10) for approx. 1 min until a fine powder was obtained and stored in sealed plastic tubes until analysis.

Saponification

The bound acetyl content of the selected samples was determined by saponification using a modified version of the method presented by Beck et al. (2018b). Wood powders (25 mg) were saponified using 1 ml of 1 M NaOH for 6 h at room temperature on a flatbed shaker. Samples (0.75 ml) of each liquid sample were recovered, neutralised with 0.375 ml of 2 M HCl and filtered through 0.45 µm syringe filters into HPLC vials. The acetic acid content of the samples was analysed by HPLC on a Shimadzu Prominence system (consisting of a LC-20AP pump, SIL-20AC autosampler, CTO-20AC column oven, and RID-10 A refractive index detector) using a Phenomenex Rezex ROA-Organic Acid H+column (7.8×300 mm, 8 µm particle size) and isocratic elution at 55 °C with 2.5 mM H_2SO_4 as the mobile phase at 0.6 ml/min. Acetic acid was quantified using refractive index detection against a calibration curve of acetic acid standards prepared in the same way as the samples.

ATR-FTIR

FTIR spectra were obtained from the selected samples using a Shimadzu IRPrestige-21 spectrometer equipped with a Specac Quest ATR accessory with a diamond crystal. Spectra were recorded in the 400–4000 cm^{-1} spectral range at a resolution of 4 cm^{-1}. Three separate spectra with 50 accumulations each were recorded for every sample. The spectral data were cut to the 800–1800 cm^{-1} range for subsequent analysis. Calibration sets were prepared by grouping the two fungi, with each group comprising the three sample types. Preprocessing of each subgroup involved

baseline correction using a third-degree polynomial subtraction ($n=3$), followed by smoothing using a Savitzky-Golay procedure (Savitzky and Golay 1964) with a second-order polynomial and a 15-point window, which effectively reduced noise while preserving the spectral features. The spectra were then subjected to unit vector normalization and mean-centring.

Partial Least Squares regression (PLSR) models (de Jong 1993) were developed for each sample type using the pre-processed calibration objects, with corresponding mass loss values as response variables. Model performance was evaluated using root mean square error of calibration (RMSEC) and cross-validation (RMSECV) at different numbers of latent variables. The cross-validation was performed by splitting the objects into five subsets, with care taken to group the similar objects (replicates) together. In each iteration, four subsets (80% of the data) were used for training, while the remaining subset (20% of the data) served as the validation set. Based on the cross-validation results, three latent variables were selected for the final model. The regression vectors of these models were compared to assess the spectral features in predicting mass loss across different fungi and sample types.

Results and discussion

The mass losses of the reference, 9% WPG and 18% WPG samples due to *C. puteana* and *R. placenta* are given in Fig. 1 as a function of sample position in the stacked-sample decay test. The two fungi and the three sample types showed substantial differences in colonisation time and mass loss pattern. *C. puteana* colonised the reference samples in 8 weeks and produced a non-linear increase in mass loss from −5% at position 1 (topmost sample) to 53% at position 6 (bottommost sample). The 9% WPG samples were also colonised rapidly (in 9 weeks) and showed a strong increase in mass loss from position 1 to position 4; however, mass loss increased more slowly from position 4 onwards, reaching only 25% at position 6. The 18% WPG samples were colonised more slowly (in 38 weeks) and showed a different mass loss pattern

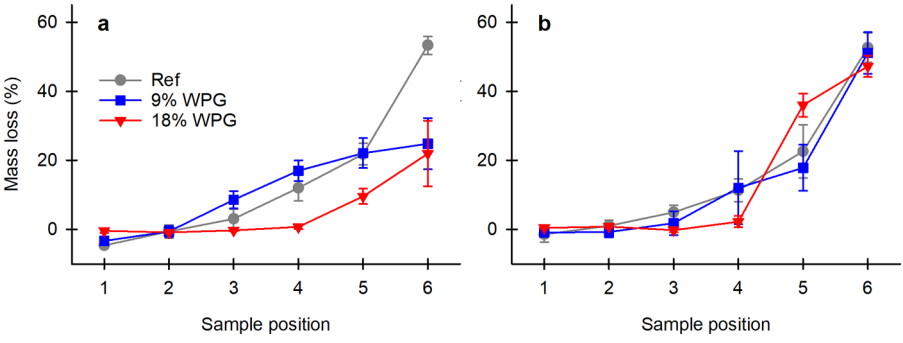

Fig. 1 Average mass losses of the reference, 9% WPG and 18% WPG samples due to *C. puteana* (**a**) and *R. placenta* (**b**) as a function of sample position in the stacked-sample decay test. The reference, 9% and 18% WPG samples were exposed to *C. puteana* for 8, 9 and 38 weeks, respectively, and to *R. placenta* for 14, 26 and 52 weeks, respectively. Error bars are ±standard deviation, $N=7$ for *C. puteana* and $N=5$ for *R. placenta*

than the 9% WPG samples: mass loss remained below 1% until position 5 and then increased to 22% at position 6. *R. placenta* colonised all three sample types more slowly than *C. puteana*. The references were colonised in 14 weeks and revealed a non-linear increase in mass loss from −1% at position 1 to 53% at position 6, while the 9% WPG samples were colonised in 26 weeks and showed a very similar mass loss pattern to the references. The 18% WPG samples on the other hand took 52 weeks to colonise and showed very little mass loss from position 1 to position 4. At position 5 the mass loss increased rapidly to 36%, followed by a more gradual increase to 47% at position 6.

The mass loss results presented in Fig. 1 confirm the findings of previous studies (Hill et al. 2006; Beck et al. 2018a, c; Thygesen et al. 2021; Ponzecchi et al. 2024) that even high WPG wood will decay if given sufficient time. However, the substantial increase in colonisation time in the high WPG samples compared to the references (from 8 to 38 weeks in the case of *C. puteana*, and from 14 to 52 weeks in the case of *R. placenta*) clearly demonstrates the increased decay resistance of acetylated wood. In the case of *C. puteana*, the acetylated samples also showed substantially reduced mass losses. Beck et al. (2018c) concluded that acetylation delays the initiation of decay by *R. placenta* but once decay begins, it proceeds at the same rate as in unmodified wood. Although degradation was not monitored over time in this experiment, the differences in mass loss pattern between the sample types suggest differences in the rate of degradation.

The decay resistance of acetylated wood is linked to its reduced moisture content, and it has been proposed that wood acetylated to sufficiently high WPG is protected from decay as the cell wall moisture content is reduced below the minimum required for the initiation of decay (Thybring 2013). The moisture contents of the unmodified and acetylated samples at the end of the decay test are shown in Fig. 2 as a function of sample position (Fig. 2a and b) and mass loss (Fig. 2c and d). Moisture content corrected for WPG due to modification and mass loss due to decay (MC*) was used to allow direct comparisons in water content between the samples without influence from changes in sample mass due to treatment or decay. Supplementary Figure S1 gives the uncorrected MCs and corrected MCs* of all individual samples. Comparison of average MCs* of the least degraded samples at position 1 (Fig. 2a and b) clearly showed the effects of acetylation: MC* was reduced from 27% in the reference samples to 20% at 9% WPG and to below 15% at 18% WPG (11% in the samples exposed to *R. placenta* and 14% in the samples exposed to *C. puteana*). MC* increased with sample position in all three sample types, most likely due to the combined effects of moisture transport from the agar and hydrolysis of the cell wall carbohydrates. The MC* of the reference samples decreased at position 6, while no decrease was seen for the acetylated samples. When MC* was plotted against mass loss (Fig. 2c and d), the MC* of the acetylated samples was seen to increase in a pattern similar to the references. All samples exposed to *C. puteana* showed a linear increase in MC* up to approx. 30% mass loss, while the samples exposed to *R. placenta* showed a rapid increase in MC* at low mass losses, particularly in the acetylated samples. Measurable mass losses were recorded in the acetylated samples at MCs* below 25%, which shows that the reduction in MC* does not protect the samples from decay. Degradation at low MCs has been previously documented in

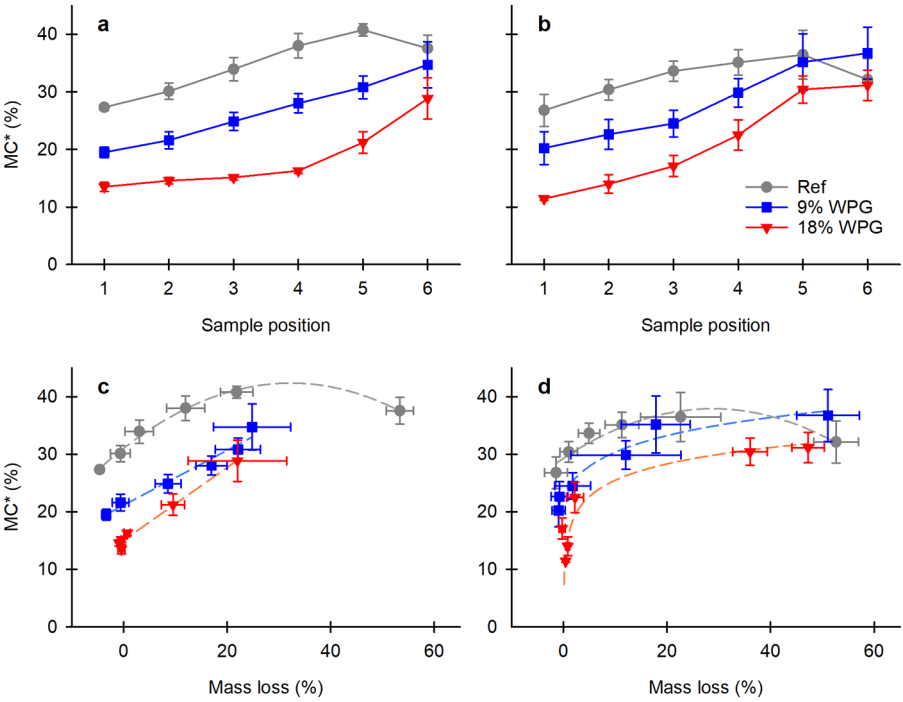

Fig. 2 Average corrected moisture content (MC*) of the reference, 9% WPG and 18% WPG samples after exposure to *C. puteana* (**a**, **c**) and *R. placenta* (**b**, **d**) as a function of sample position (**a**, **b**) and mass loss (**c**, **d**). The reference, 9% and 18% WPG samples were exposed to *C. puteana* for 8, 9 and 38 weeks, respectively, and to *R. placenta* for 14, 26 and 52 weeks, respectively. Error bars are ±standard deviation, $N=7$ for *C. puteana* and $N=5$ for *R. placenta*

both modified and unmodified wood in the presence of an external moisture source (Meyer et al. 2016; Brischke and Alfredsen 2020).

To investigate the role of deacetylation in the degradation of acetylated wood, a subset of samples was selected from every sample group and their acetyl contents determined by saponification. The post-decay acetyl contents of the samples are given in Fig. 3 as a function of mass loss. The unacetylated reference samples contained a small concentration of acetyl groups due to the natural acetylation of hemicelluloses (Fengel and Wegener 1989). The acetyl content of the references was around 1.5% in the least decayed samples and decreased gradually with increasing mass loss due to both *C. puteana* and *R. placenta* as a result of hemicellulose degradation. The acetylated samples showed substantial variation in their acetyl content, which is not surprising given that there were substantial variations in their gravimetrically determined acetylation degree (see Supplementary Table S2). The acetyl content of the 9% WPG samples showed little change as a function of mass loss due to either fungus, indicating that no preferential deacetylation of the material took place over the course of decay. The 18% WPG samples exposed to *C. puteana* showed a very slight decreasing trend as a function of mass loss, while the samples exposed to *R. placenta* revealed a small, rapid decrease at low mass losses. No consistent decrease in acetyl

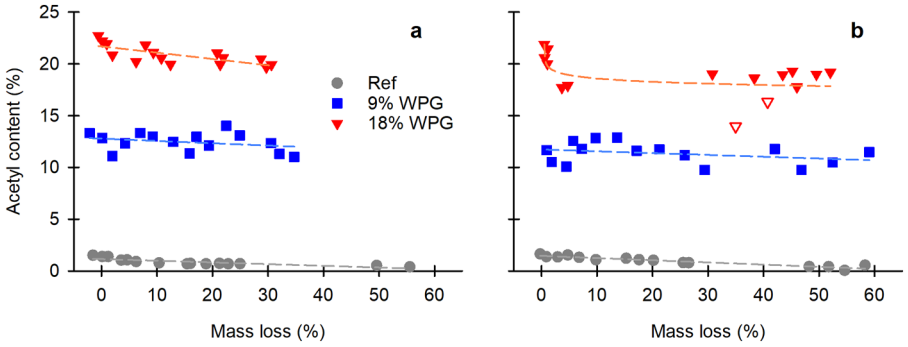

Fig. 3 Acetyl contents of selected reference, 9% WPG and 18% WPG samples after exposure to *C. puteana* (**a**) and *R. placenta* (**b**) as a function of mass loss. Two 18% WPG samples exposed to *R. placenta* (marked with open symbols) showed reduced acetyl content compared to the other samples

content was seen at higher mass losses due to *R. placenta*, but 2 of the 15 samples selected for saponification were found to have lower acetyl contents than the other samples (14.0 and 16.3%). The gravimetrically determined WPGs of the samples in question were not lower than the WPGs of the other samples (see Supplementary Table S2), which indicates that the samples had been deacetylated by the fungus.

The acetyl content data showed that *C. puteana* caused little to no preferential deacetylation of acetylated wood, while the small decrease seen in the 18% WPG samples exposed to *R. placenta* indicated that *R. placenta* may have caused slight preferential deacetylation in highly acetylated wood in the early stages of decay. Although the decrease seen in the 18% WPG samples was small, the identified trend is consistent with previous findings. Preferential deacetylation by *R. placenta* in the early stages of decay was recorded by Beck et al. (2018c), although the extent of deacetylation observed by them was higher than in this experiment, possibly due to the use of more highly acetylated samples by Beck et al. Deacetylation of acetylated wood by *C. puteana* has not been previously investigated, and the results presented here indicate that the two fungal species may differ in their mechanisms of degradation. These differences can also be seen in the MC* data (Fig. 2), where the initial deacetylation by *R. placenta* may explain the rapid increase in MC* seen in the acetylated samples. The initial deacetylation may be due to targeted removal of acetyl groups by the fungus or to the action of the Fenton-based oxidative system used by brown rot fungi in the early stages of decay. Gene expression studies have shown that acetylation prolongs the expression of genes involved in oxidative degradation and delays the expression of hydrolytic enzymes (Beck et al. 2018a). It is impossible to say which mechanism is involved based on the present data, but the fact that deacetylation was only seen in the 18% WPG samples suggests that the deacetylation is specific to highly acetylated wood. Regardless of the mechanism of deacetylation, it is clear that extensive deacetylation is not necessary for degradation of acetylated wood by either fungus.

Apart from the preferential deacetylation seen in the 18% WPG samples by *R. placenta*, the acetyl content of the samples showed little change as a function of mass loss, indicating that acetyl groups were lost from the wood at the same rate as cell

wall polymers. Although lignin is more extensively acetylated than carbohydrates, a significant portion of the acetyl groups are found on the carbohydrate fraction (Rowell et al. 1994), and the degradation of the acetylated carbohydrates by the fungi is bound to cause a loss in acetyl groups. However, it is unclear if the loss of acetyl groups is exclusively due to the degradation of acetylated carbohydrates by the fungi or if the carbohydrates or lignin are also deacetylated over the course of decay. Furthermore, although the data indicate that acetyl groups are lost from acetylated wood at the same rate as cell wall polymers, the bulk measurements performed here do not rule out the possibility of preferential deacetylation before polymer degradation on a more localised level. Acetyl groups interfere with the action of hydrolytic enzymes, necessitating their removal for the efficient hydrolysis of carbohydrates to digestible monosaccharides (Puls 1997). Acetylation has also been shown to reduce wood degradation by Fenton reagent in laboratory degradation experiments, most likely due to reduced iron diffusion (Hosseinpourpia and Mai 2016). If the action of Fenton chemistry is substantially impeded under real brown rot degradation conditions as well, the removal of acetyl groups may be necessary for the initiation of decay. Potential acetylation gradients in the cell wall, which can occur when acetylation is performed in neat acetic anhydride (Mäkelä et al. 2021), may further increase or decrease the need for localised deacetylation.

To investigate the degradation of acetylated wood in more detail, ATR-FTIR spectra were collected from the samples selected for acetyl content measurements. The average spectra of the samples with minimum mass loss are given in Fig. 4a, while Fig. 4b, c and d give the average spectra of the minimum and maximum mass loss reference, 9% WPG and 18% WPG samples, respectively. Individual replicate spectra are shown in Supplementary Figure S3. The minimum mass loss spectra clearly showed the effects of acetylation as increased band intensity at 1225, 1369 and 1738 cm^{-1}, in agreement with previous reports (Schwanninger et al. 2011; Thygesen et al. 2021; Ponzecchi et al. 2024). In the unmodified reference samples, degradation by both *C. puteana* and *R. placenta* caused a decrease in band intensity at 1056, 1107, 1317, and 1369 cm^{-1}. These bands are derived from the C–O valence vibration of carbohydrates, ring asymmetric valence vibration of carbohydrates, CH_2 rocking vibration of cellulose, and C–H deformation of cellulose, respectively (Pandey 1999; Schwanninger et al. 2004; Fackler et al. 2010). Strong band intensity increases were seen at 1219, 1265 and 1508 cm^{-1}, corresponding to the G-ring C–C plus C–O plus C=O stretch of lignin, G-ring plus C=O stretch of lignin, and aromatic skeletal vibrations of lignin, respectively (Faix 1991; Pandey 1999; Schwanninger et al. 2004; Fackler et al. 2010). Intensity increases were also seen in other lignin-derived bands: aromatic C–H deformation at 1138 cm^{-1}, and aromatic skeletal vibrations plus C=O stretch at 1597 cm^{-1} (Faix 1991; Schwanninger et al. 2004; Fackler et al. 2010). An increase was also seen at 1726 cm^{-1}, tentatively assigned to unconjugated C=O stretch of lignin (Faix 1991; Schwanninger et al. 2004). These band intensity changes are consistent with preferential carbohydrate degradation and the resulting increase in residual lignin content. Brown rot decay also causes lignin modification as the hydroxyl radicals generated by the Fenton reaction cause sidechain cleavage, demethylation, and oxidation, giving an increase in aromatic content, OH content, and C=O content (Filley et al. 2002; Yelle et al. 2011); the changes seen in the lignin-

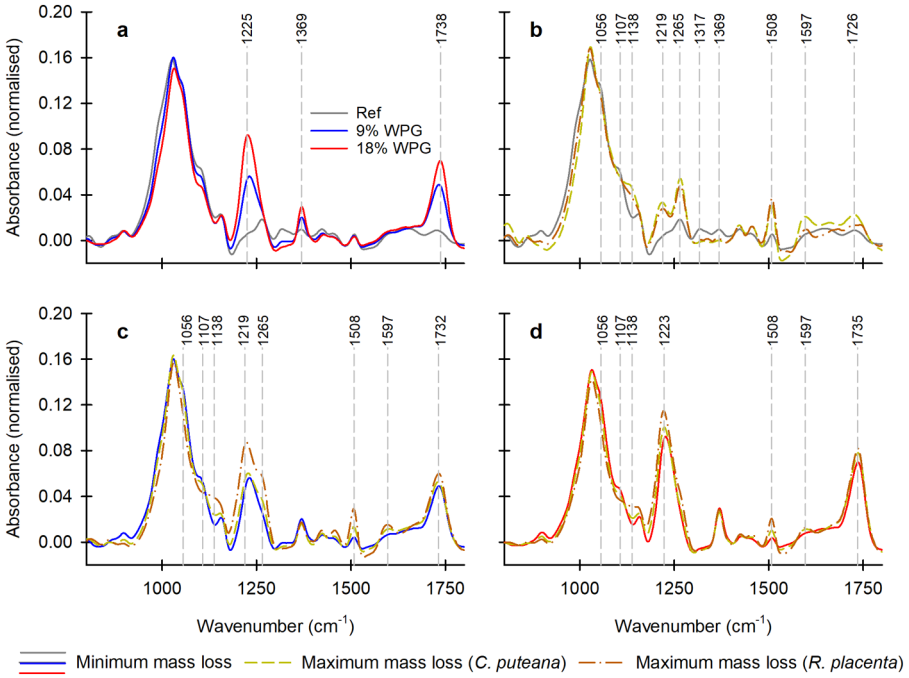

Fig. 4 Average ATR-FTIR spectra of the reference, 9% WPG and 18% WPG samples with minimum mass loss (**a**), and average FTIR spectra of the reference (**b**), 9% WPG (**c**) and 18% WPG (**d**) samples with minimum mass loss and maximum mass loss due to *C. puteana* and *R. placenta*

derived bands are consistent with extensive lignin modification. The spectra of the acetylated samples degraded by *C. puteana* and *R. placenta* were still dominated by the acetylation-related bands, as expected given the lack of extensive deacetylation (Fig. 3). Many of the spectral changes seen in the reference samples could be seen in the acetylated samples as well, which means that the samples were degraded by a similar mechanism to the references.

To gain more insight into potential differences in degradation between the sample types, the ATR-FTIR spectral data were analysed by PLSR. Separate models were built for the different wood-fungus combinations to understand which spectral changes are associated with mass loss in the different samples. The regression vectors are shown in Fig. 5. All models were built using three latent variables as the objective was to obtain chemical information. RMSEC, RMSECV, and plots of observed vs. predicted mass loss are shown in Supplementary Figure S4. In the samples degraded by *C. puteana*, mass loss was associated with increased intensity at 1026, 1144, 1194, 1273, 1508, and 1589 cm^{-1}, and decreased intensity at 1070, 1169, and 1317 cm^{-1}. The positive bands were assigned to lignin. The 1144, 1273, 1508, and 1589 cm^{-1} bands were assigned to aromatic C–H deformation, G-ring plus C=O stretch, aromatic skeletal vibrations, and aromatic skeletal vibrations plus C=O stretch as discussed above. The 1026 cm^{-1} band was assigned to aromatic C–H in-plane deformation plus C–O in primary alcohols plus C=O stretch (Faix 1991; Pandey 1999). The 1194 cm^{-1} band could not be identified but is likely to be lignin-derived as

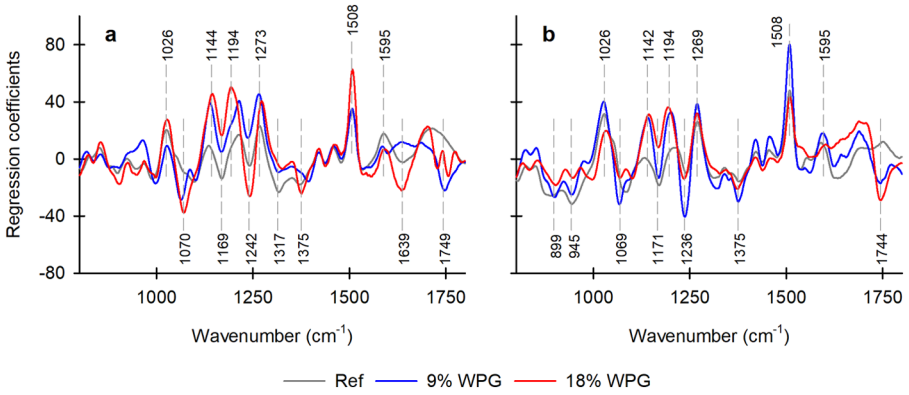

Fig. 5 Regression coefficients of PLSR models predicting mass loss in the reference, 9% WPG and 18% WPG samples degraded by *C. puteana* (**a**) and *R. placenta* (**b**)

well. The negative bands were assigned to carbohydrates. The bands at 1070 and 1317 cm^{-1} were assigned to the C–O valence vibration of carbohydrates and the CH_2 rocking vibration of cellulose as discussed above. The 1169 cm^{-1} band was tentatively assigned to the C–O–C asymmetric valence vibration of carbohydrates (Pandey 1999; Schwanninger et al. 2004; Fackler et al. 2010); lignin-derived bands have been found in this region but not in softwood lignin (Faix 1991). In the samples degraded by *R. placenta*, positive coefficients were seen for the lignin-derived bands at 1026, 1142, 1194, 1269, 1508, and 1597 cm^{-1}, and negative coefficients for the carbohydrate-derived bands at 1070 and 1169 cm^{-1}. Additional negative bands were seen at 889 and 945 cm^{-1}, derived from the C–H deformation of cellulose and from the pyran ring, respectively (Schwanninger et al. 2004; Fackler et al. 2010). In the case of both fungi, negative coefficients were seen for the acetylation-derived bands at 1242, 1375, and 1749 cm^{-1}, showing that acetyl groups were lost from the samples. This finding is in agreement with the acetyl content data (Fig. 3), which indicated that acetyl groups were lost over the course of decay at the same rate as the wood cell wall polymers.

Even though the PLSR analysis showed that mass loss was associated with carbohydrate degradation and lignin accumulation in all samples, substantial differences in the regression vectors could be seen between the sample types. In the samples degraded by *C. puteana*, the carbohydrate C–O band at 1070 cm^{-1} showed large negative regression coefficients in the acetylated samples but not the references, while the tentative carbohydrate C–O–C band at 1169 cm^{-1} as well as the cellulose CH_2 band at 1317 cm^{-1} showed negative coefficients in the references but not the acetylated samples. Lignin-derived bands also showed differences between the sample types; the 1144 cm^{-1} band assigned to aromatic C–H and the 1194 cm^{-1} band tentatively assigned to phenolic OH (Derkacheva and Sukhov 2008) displayed much larger positive regression coefficients in the acetylated samples than the references. In the samples degraded by *R. placenta*, the cellulose band at 889 cm^{-1} and pyran ring band at 945 cm^{-1} had more negative regression coefficients in the references than in the acetylated samples, while the lignin aromatic C–H band at 1142 cm^{-1} and

the lignin phenolic OH band at 1994 cm^{-1} had more positive coefficients in the acetylated samples than the references. The carbohydrate bands at 1069 and 1171 cm^{-1} had more negative coefficients in the reference and 9% WPG samples than the 18% WPG samples.

The differences in regression vectors suggest differences in degradation patterns between the sample types. However, the differences may also be influenced by differences in decay stage. Decay stage is likely to be a factor at least in the case of *C. puteana*, where the reference samples had a maximum mass loss of 56%, while the 9% and 18% WPG samples had maximum mass losses of only 35 and 31%, respectively. Decay stage is likely to be less influential in the case of *R. placenta*, where the maximum mass loss in all sample types was over 50% (58, 59 and 52% for the reference, 9% WPG and 18% WPG samples, respectively). The differences in the regression coefficients of the carbohydrate-derived bands may reflect differences in patterns of carbohydrate degradation caused by acetylation of the carbohydrates, while the differences related to lignin-derived bands may reflect differences in lignin modification. The strong association of the aromatic C–H band at 1142 cm^{-1} and the phenolic OH band at 1194 cm^{-1} with mass loss in acetylated wood may be indicative of more extensive sidechain cleavage and demethylation in the acetylated samples as a result of hydroxyl radical attack. However, the aromatic ring bands at 1508 and 1597 cm^{-1} did not show consistently higher coefficients in the acetylated samples, and the aromatic C–H plus C–O plus C=O band at 1026 cm^{-1} and the G ring plus C=O band at 1269 cm^{-1} did not show substantial differences between the reference and acetylated samples either, suggesting a lack of difference in lignin aromatic content and C=O content between the sample types. The increased phenolic OH content seen in the acetylated samples may instead be due to lignin deacetylation, which would cause an increase in phenolic OH without an increase in aromatic C=O. However, the degradation (rather than deacetylation) of acetylated lignin is also possible. Regardless of the exact mechanism, the finding suggests that the loss of acetyl groups over the course of decay is not only due to degradation of acetylated carbohydrates. Finally, the acetylation related bands at 1242, 1375 and 1749 cm^{-1} also showed differences between sample types. Although all three bands had negative coefficients in the acetylated samples degraded by both fungi, the different bands showed different behaviours in the 9% and 18% WPG samples. However, these differences are likely due to the fact that the bands also receive contributions from the wood cell wall polymers in addition to acetyl groups rather than due to differences in the chemistry of deacetylation.

Conclusion

The stacked-sample decay test showed that acetylated wood could be degraded to high mass losses by *C. puteana* and *R. placenta* despite the strong reduction in moisture content under decay test conditions. Post-decay acetyl content measurements showed little to no preferential deacetylation of the acetylated samples by *C. puteana*, while slight deacetylation of high WPG wood by *R. placenta* was seen in the early stages of decay. The fact that deacetylation was seen only in the high WPG samples

suggests that the deacetylation, regardless of its exact mechanism, is specific to high WPG wood. FTIR analysis of the decayed samples showed that both fungi degraded the reference and acetylated wood by a typical brown rot mechanism characterised by preferential carbohydrate degradation and lignin modification. Despite the similarities, PLSR analysis of the spectral data revealed some differences between the reference and acetylated samples in carbohydrate degradation and lignin modification. The spectral data suggested that the fungi caused the loss of acetyl groups in lignin, which means that the deacetylation seen in the samples exposed to *R. placenta* is not only due to the degradation of acetylated carbohydrates. The degradation of acetylated wood and the mechanisms of deacetylation require further investigation.

Supplementary Information The online version contains supplementary material available at https://doi.org/10.1007/s00226-024-01620-8.

Author contributions Tiina Belt: Conceptualization; Funding acquisition; Investigation; Methodology; Visualization; Writing - original draft; Writing - review & editing. Muhammad Awais: Formal analysis; Software; Writing - review & editing.

Funding Open access funding provided by Natural Resources Institute Finland. This work received funding from the Research Council of Finland (grant no. 330087 and 349198), from the Finnish Cultural Foundation (grant no. 00240121) and from Tutkijat Maailmalle (grant no. 20240032).

Data availability The datasets generated and analysed during the current study are available in the Zenodo repository at https://doi.org/10.5281/zenodo.12570844.

Declarations

Ethical approval Not applicable.

Competing interests The authors declare no competing interests.

References

Beck G, Hegnar OA, Fossdal CG, Alfredsen G (2018a) Acetylation of Pinus radiata delays hydrolytic depolymerisation by the brown-rot fungus rhondonia placenta. Int Biodeter Biodegrad 135:39–52. https://doi.org/10.1016/j.ibiod.2018.09.003

Beck G, Strohbusch S, Larnøy E et al (2018b) Accessibility of hydroxyl groups in anhydride modified wood as measured by deuterium exchange and saponification. Holzforschung 72:17–23. https://doi.org/10.1515/hf-2017-0059

Beck G, Thybring EE, Thygesen LG (2018c) Brown-rot fungal degradation and de-acetylation of acetylated wood. Int Biodeter Biodegrad 135:62–70. https://doi.org/10.1016/j.ibiod.2018.09.009
Beck G, Thybring EE, Thygesen LG, Hill C (2018d) Characterization of moisture in acetylated and propionylated radiata pine using low-field nuclear magnetic resonance (LFNMR) relaxometry. Holzforschung 72:225–233. https://doi.org/10.1515/hf-2017-0072
Belt T, Awais M, Mäkelä M (2022) Chemical characterization and visualization of Progressive Brown Rot Decay of Wood by Near Infrared Imaging and Multivariate Analysis. Front Plant Sci 13:940745. https://doi.org/10.3389/fpls.2022.940745
Brischke C, Alfredsen G (2020) Wood-water relationships and their role for wood susceptibility to fungal decay. Appl Microbiol Biotechnol 104:3781–3795. https://doi.org/10.1007/s00253-020-10479-1
Čermák P, Baar J, Dömény J et al (2022) Wood-water interactions of thermally modified, acetylated and melamine formaldehyde resin impregnated beech wood. Holzforschung 76:437–450. https://doi.org/10.1515/hf-2021-0164
de Jong S (1993) SIMPLS: an alternative approach to partial least squares regression. Chemometr Intell Lab Syst 18:251–263. https://doi.org/10.1016/0169-7439(93)85002-X
Derkacheva O, Sukhov D (2008) Investigation of Lignins by FTIR Spectroscopy. Macromol Symp 265:61–68. https://doi.org/10.1002/masy.200850507
Digaitis R, Thybring EE, Thygesen LG, Fredriksson M (2021) Targeted acetylation of wood: a tool for tuning wood-water interactions. Cellulose 8009–8025. https://doi.org/10.1007/s10570-021-04033-z
Fackler K, Stevanic JS, Ters T et al (2010) Localisation and characterisation of incipient brown-rot decay within spruce wood cell walls using FT-IR imaging microscopy. Enzyme Microb Technol 47:257–267. https://doi.org/10.1016/j.enzmictec.2010.07.009
Faix O (1991) Classification of Lignins from different Botanical origins by FT-IR Spectroscopy. 45:21–28. https://doi.org/10.1515/hfsg.1991.45.s1.21
Fengel D, Wegener G (1989) Wood: chemistry, ultrastructure, reactions. Walter de Gruyter, Berlin
Filley TR, Cody GD, Goodell B et al (2002) Lignin demethylation and polysaccharide decomposition in spruce sapwood degraded by brown rot fungi. Org Geochem 33:111–124. https://doi.org/10.1016/S0146-6380(01)00144-9
Fredriksson M, Digaitis R, Engqvist J, Thybring EE (2024) Effect of targeted acetylation on wood–water interactions at high moisture states. Cellulose 31:869–885. https://doi.org/10.1007/s10570-023-05678-8
Hill CAS (2006) Wood Modification: Chemical, Thermal and other processes. John Wiley & Sons, Ltd.
Hill CAS, Forster SC, Farahani MRM et al (2005) An investigation of cell wall micropore blocking as a possible mechanism for the decay resistance of anhydride modified wood. Int Biodeter Biodegrad 55:69–76. https://doi.org/10.1016/j.ibiod.2004.07.003
Hill CAS, Hale MD, Ormondroyd GA et al (2006) Decay resistance of anhydride-modified corsican pine sapwood exposed to the brown rot fungus Coniophora Puteana. Holzforschung 60:625–629. https://doi.org/10.1515/HF.2006.105
Himmel S, Mai C (2015) Effects of acetylation and formalization on the dynamic water vapor sorption behavior of wood. Holzforschung 69:633–643. https://doi.org/10.1515/hf-2014-0161
Hosseinpourpia R, Mai C (2016) Mode of action of brown rot decay resistance of acetylated wood: resistance to Fenton's reagent. Wood Sci Technol 50:413–426. https://doi.org/10.1007/s00226-015-0790-0
Mäkelä M, Altgen M, Belt T, Rautkari L (2021) Hyperspectral imaging and chemometrics reveal wood acetylation on different spatial scales. J Mater Sci 56:5053–5066. https://doi.org/10.1007/s10853-020-05597-0
Meyer L, Brischke C, Treu A, Larsson-Brelid P (2016) Critical moisture conditions for fungal decay of modified wood by basidiomycetes as detected by pile tests. Holzforschung 70:331–339. https://doi.org/10.1515/hf-2015-0046
Pandey KK (1999) A study of chemical structure of soft and hardwood and wood polymers by FTIR spectroscopy. J Appl Polym Sci 71:1969–1975
Papadopoulos AN, Hill CAS (2003) The sorption of water vapour by anhydride modified softwood. Wood Sci Technol 37:221–231. https://doi.org/10.1007/s00226-003-0192-6
Ponzecchi A, Alfredsen G, Fredriksson M et al (2024) Localization and characterisation of brown rot in two types of acetylated wood. Cellulose 1875–1890. https://doi.org/10.1007/s10570-023-05680-0
Puls J (1997) Chemistry and biochemistry of hemicelluloses: relationship between hemicellulose structure and enzymes required for hydrolysis. Macromol Symp 120:183–196. https://doi.org/10.1002/masy.19971200119

Ringman R, Pilgård A, Brischke C, Richter K (2014) Mode of action of brown rot decay resistance in modified wood: a review. Holzforschung 68:239–246. https://doi.org/10.1515/hf-2013-0057
Ringman R, Pilgård A, Brischke C et al (2017) Incipient brown rot decay in modified wood: patterns of mass loss, structural integrity, moisture and acetyl content in high resolution. Int Wood Prod J 8:172–182. https://doi.org/10.1080/20426445.2017.1344382
Ringman R, Beck G, Pilgård A (2019) The importance of moisture for Brown Rot Degradation of Modified Wood: a critical discussion. Forests 10:522. https://doi.org/10.3390/f10060522
Rowell RM, Simonson R, Hess S et al (1994) Acetyl distribution in Acetylated Whole Wood and reactivity of isolated Wood Cell-Wall Components to Acetic Anhydride. Wood Fiber Sci 11–18
Savitzky Abraham, Golay MJE (1964) Smoothing and differentiation of data by simplified least squares procedures. Anal Chem 36:1627–1639. https://doi.org/10.1021/ac60214a047
Schwanninger M, Rodrigues JC, Pereira H, Hinterstoisser B (2004) Effects of short-time vibratory ball milling on the shape of FT-IR spectra of wood and cellulose. Vib Spectrosc 36:23–40. https://doi.org/10.1016/j.vibspec.2004.02.003
Schwanninger M, Stefke B, Hinterstoisser B (2011) Qualitative Assessment of Acetylated Wood with Infrared Spectroscopic methods. J Near Infrared Spectrosc 19:349–357. https://doi.org/10.1255/jnirs.942
Thybring EE (2013) The decay resistance of modified wood influenced by moisture exclusion and swelling reduction. Int Biodeter Biodegrad 82:87–95. https://doi.org/10.1016/j.ibiod.2013.02.004
Thybring EE, Piqueras S, Tarmian A, Burgert I (2020) Water accessibility to hydroxyls confined in solid wood cell walls. Cellulose 27:5617–5627. https://doi.org/10.1007/s10570-020-03182-x
Thygesen LG, Engelund ET, Hoffmeyer P (2010) Water sorption in wood and modified wood at high values of relative humidity. Part I: results for untreated, acetylated, and furfurylated Norway spruce. Holzforschung 64:315–323. https://doi.org/10.1515/hf.2010.044
Thygesen LG, Beck G, Nagy NE, Alfredsen G (2021) Cell wall changes during brown rot degradation of furfurylated and acetylated wood. Int Biodeter Biodegrad 162:105257. https://doi.org/10.1016/j.ibiod.2021.105257
Yelle DJ, Wei D, Ralph J, Hammel KE (2011) Multidimensional NMR analysis reveals truncated lignin structures in wood decayed by the brown rot basidiomycete Postia placenta. Environ Microbiol 13:1091–1100. https://doi.org/10.1111/j.1462-2920.2010.02417.x
Zelinka SL, Ringman R, Pilgård A et al (2016) The role of chemical transport in the brown-rot decay resistance of modified wood. Int Wood Prod J 7:66–70. https://doi.org/10.1080/20426445.2016.1161867